

Colour development of red perovskite pigment $Y(\text{Al},\text{Cr})\text{O}_3$ in various ceramic applications

F. Matteucci^{*1}, C. Lepri Neto², M. Dondi¹, G. Cruciani³, G. Baldi⁴, A.O. Boschi²

¹*Institute of Science and Technology for Ceramics (CNR-ISTEC), Via Granarolo 64, 48018 Faenza (Italy)*

—dondi@istec.cnr.it

²*Laboratório de Revestimentos Cerâmicos (LaRC) - Universidade Federal de São Carlos, 13565-905 São Carlos SP (Brazil)*

—daob@power.ufscar.br

³*Earth Science Department, Corso Ercole I d'Este 32, University of Ferrara, 44100 Ferrara (Italy)*

—cruc@unife.it

⁴*Colorobbia Italia SpA, Advanced Research Laboratories, Via Pietramarina 123, 50023 Sovigliana Vinci (Italy)*

—baldig@colorobbia.it

Abstract

Ceramic pigments based on the perovskite structure develop a promising red hue and furthermore present no environmental or health care problems. Pigment colouring efficiency was tested in different ceramic applications, both through-body and glazes. Final products, fired varying both the maximum temperature and soaking time, were characterized by the colourimetric point of view. Research efforts were focused both on the factors and on the mechanism mainly influencing perovskite dissolution by calculating the phase composition of different ceramic matrices and by observing the pigment microstructure. Furthermore, pigment powders were characterized by a structural and spectroscopic point of view. The pigment dissolution is slightly affected by the firing cycle and mostly governed by amount and chemical composition of the liquid phase. In particular, the larger the content of chemically aggressive components - such as calcium, magnesium, zinc and lead oxides - the strongest and faster the pigment dissolution.

Keywords: ceramic glazes, ceramic pigment, colorimetric characterization, perovskite, porcelain stoneware, yttrium aluminate.

Introduction

The development of pigments imparting an intense red shade to both ceramic bodies and glazes, is a worldwide pressing task and one of the most updated field of research.¹⁻² In fact, current industrial red ceramic pigments do not fulfil all the needed requirements of the whole ceramic production, due to the environmental, technological or colouring problems.³

^{*}Corresponding author: e-mail: matteucci@istec.cnr.it

Concerning the ceramic application of the incomparable yellow-orange-red colours of the greenockite-cadmoseelite solid solution ($\text{CdSe}_{1-x}\text{S}_x$), the problems are either technological, as it is not stable in high-temperature firing applications, or environmental, due to the high toxicity of cadmium and selenium. In order to overcome the greenockite-cadmoseelite technological problems, an inclusion technology of cadmium sulpho-selenide inside zircon has been developed, but it brings about a high cost pigment.⁴⁻⁵

The other red-coloured ceramic pigments available on the market display hues far away from the pure red. The malayaite pigment ($\text{CaSn}_{1-x}\text{Cr}_x\text{SiO}_5$) gives a magenta colour, while zircon-hematite ($\text{ZrSiO}_4+\text{Fe}_2\text{O}_3$) shows a red-peach or coral-like hue and corundum ($\text{Al}_{2-x-y}\text{Mn}_x\text{Cr}_y\text{O}_3$) is pink.⁶⁻⁸

A brand new ceramic pigment – $\text{YAl}_{1-x}\text{Cr}_x\text{O}_3$ where $0.03 < x < 0.12$ – obtained through conventional ceramic processing, was patented in 1996.⁹ This yttrium aluminate doped with chromium presents no environmental or health care problems, as the raw materials and final compound are non toxic.¹⁰⁻¹² This pigment ensures the most intense red hue together with the highest colour purity among all the red-coloured ceramic pigments, after the greenockite-cadmoseelite solid solution.¹³⁻¹⁴

The yttrium aluminate pigment, crystallizing with the perovskite structure of type $\text{A}^{\text{III}}\text{B}^{\text{III}}\text{O}_3$, is characterised by a trivalent cation in both crystallographic positions:¹⁵

- A is a cubo-octahedral site, enclosed in a cage formed by eight BX_6 polyhedra, that hosts Y in 8-fold coordination;¹⁶
- B is an octahedral site sharing all of its corners with the neighbouring octahedra and hosting Al^{3+} partially substituted by Cr^{3+} .

This chromium doping is the origin of red colour of the pigment, due to the absorption of the green-blue-violet range of the visible spectrum. In particular, this absorption is related to the strong crystal field effect of the YAlO_3 perovskite structure.^{12,17} Furthermore, this structure gives the pigment a high refractory character (melting point $\sim 1950^\circ\text{C}$) and good optical properties, such as high refractive indices and a satisfactory stability in silicatic matrices, such as the ceramic ones.¹⁰

This work aims at the evaluation of the technological performance of the red perovskite pigment in different ceramic glazes and bodies. The parameters that mostly influence the chromatic efficiency of perovskite in different ceramic applications, as the pigment dissolution in the liquid phase, will be studied. Technological tests were performed adding the pigment to several porcelain stoneware bodies as well as ceramic frits and glazes. The colour, phase composition, amount of undissolved pigment, and the microstructural evolution of grain boundaries between pigment particles and glassy phase will be assessed.

Experimental procedure

Sample preparation

The current industrial production involves dosing and mixing of raw materials (oxides, carbonates, etc.), dry or wet milling, calcining, washing, drying and powder deagglomeration.² In this investigation, two perovskite pigments were used:

1. an industrial product achieved by adding a filler (40% wt. of quartz) to calcined perovskite with $\text{YAl}_{0.965}\text{Cr}_{0.035}\text{O}_3$ stoichiometry¹⁸, used for the technological characterization and particle size measurements;

2. a pigment of the same stoichiometry, prepared using reagent-grade Y_2O_3 , Al_2O_3 and Cr_2O_3 , plus 1% in weight of mineralizers (calcium and sodium fluorides and carbonates) that underwent the structural investigation by X-rays diffraction and diffuse reflectance spectroscopy; the mixture was ground in a porcelain jar-mill with Alubit[®] balls, then dried and fired up to 1500°C with a firing cycle of 15 hours and 1 hour soaking.

Characterisation methods

The structural investigation of the prepared pigment was carried out through high resolution X-ray powder diffraction (HR-XRPD), performed at the Swiss-Norwegian Beam Lines of the European Synchrotron Radiation Facility (Grenoble, France). Powder samples, filled in 0.3 mm glass capillaries, were mounted in the Debye-Scherrer geometry and axially spun during measurement. The wavelength was set to $\lambda = 0.79998 \text{ \AA}$ and data were collected at room temperature in the 1-52.5° range.

The crystal structure Rietveld refinement was performed using the GSAS-EXPGUI package.^{19,20} Starting atomic parameters for the orthorhombic perovskite YAIO₃ were taken from Diehl and Brandt,²¹ adopting the same Pnma non-standard setting. Refined variables were: scaling factors, zero-point correction, cell dimensions, 10 coefficients of the shifted Chebyshev function to fit the background, atomic positions, and profile coefficients: 3 gaussian (GU, GV, and GW) and 2 lorentzian terms (Lx and Ly). The Rietveld refinement fit of the sample is shown in Figure 1.

Pigment were then characterised with the UV-visible-NIR spectrophotometer (Perkin-Elmer, λ 35, 300-1100 nm range, step 0.3 nm) equipped with an integrating sphere made of BaSO₄. Measurements were performed with diffuse reflectance method using BaSO₄ as reference and CIELab coordinates were calculated by the spectra with standard illuminant D₆₅ and observer 10°.

The particle size distribution (PSD) of the industrial pigment was measured by X-rays monitoring of gravity sedimentation with a Micromeritics Sedigraph 5100 (ASTM C 958).

Technological tests were carried out adding the industrial pigment (5% wt. corresponding to 3% wt. of perovskite) to different ceramic bodies, glazes and frits, whose chemical compositions and physical properties²²⁻²³ are reported in Tables 1 and Table 2 respectively. In particular, the pigment was introduced into:

- three porcelain stoneware bodies (BA=conventional, SB=ultrawhite and TL=translucid);
- two frits for double-fired wall tiles (F1 and F2) and three glazes (S1 for porcelain stoneware tiles, S2 for single-fired, light-coloured stoneware tiles, and S3 for *monoporosa* wall tiles).

All samples were fired in an electrical roller kiln with a firing cycle of 51 minutes. The firing temperature of the bodies and the softening temperature for frits and glazes were determined using hot stage microscopy.²⁴

In order to investigate the kinetics of pigment dissolution in the various ceramic matrices, samples were fired at different temperatures (Table 3) for different soaking times (5, 15 or 45 minutes).

The technological performance of the perovskite pigment was characterized by measuring:

- colour by diffuse reflectance spectroscopy (DRS) using a HunterLab Miniscan XE Plus spectrophotometer in the 380-780 nm range, using a white glazed tile (x=0.315; y=0.333) as reference and CIELab coordinates were calculated by the spectra with standard illuminant D₆₅ and observer 10°.
- Amount of undissolved pigment and phase composition of both porcelain stonewares and glazes were determined by XRPD with a Rigaku *Dmax III C* diffractometer (20-50 ° 2 θ range; Δ 2 θ step 0.02°; 4 s per step); the quantitative interpretation of XRPD patterns was performed using the internal standard method (CaF₂ as reference).
- Microstructure of pigment using SEM (Cambridge Stereoscan 360) attached with EDS electron microprobe (Link Analytical).

Results and discussion

Pigment properties

The prepared pigment contains a small amount of impurity phases such as fluorite, yttrium aluminum oxide and yttrium oxyfluoride (total fraction 5.8 wt %) besides the yttrium aluminate perovskite. The structure refinement shows that Cr-doped perovskite has an orthorhombic symmetry and crystallizes in the *Pnma* space group. Refined unit-cell parameters and crystallographic details are given in table 4. The Al vs. Cr atomic fractions in the octahedral B site were determined by refining the relative contribution of the Al/Cr scattering factors assuming a full occupancy of the B site. The refined Cr fraction (0.029) is in relatively good agreement with that inferred from the batch composition (0.035) (estimated accuracy is about 0.01). The refined cell parameters and bond distances of the studied Cr-doped perovskite show only small differences with respect to the undoped YAIO_3 .²¹ The cell volume of the former (203.91 \AA^3) is slightly larger than the latter (203.62 \AA^3) confirming the Cr (0.62 Å) to Al (0.54 Å) substitution. The same effect is not evident by comparing the average of refined octahedral bond distances of the two structures; however, it should be pointed out that the expected linear increase in the average octahedral bond distance due to incorporation of a 0.03 Cr fraction in the B site is of about 0.002 \AA which is within the absolute experimental error on the refined distances. As far as the UV-Vis-NIR spectra are concerned, the red colour developed by the perovskite pigment ($a^*=23.5$) is due to the strong absorption band in the 350-650 nm range. This strong absorption in the green-blue-violet range of the visible spectrum is due to the coalescence of the two Cr^{3+} peaks linked with lowering the point symmetry in the orthorhombic perovskites (Fig. 2B).²⁵

The behaviour of the pigment into a glaze or a body is deeply affected by the particle size distribution. There is a difficult compromise between the largest size getting a suitable dispersion and preventing from spotting effects, and the finest size avoiding a significant dissolution.²⁶ In the current case, the median diameter of the pigment (d_{50}) is $3 \mu\text{m}$ and curve shows more than the 50% of the pigment particles are in the $3-10 \mu\text{m}$ range (Fig. 2A).

3.2. Technological behaviour

Colour development in porcelain stoneware bodies

The red colour of the different porcelain stonewares decreased for increasing soaking time: slightly in the case of BA and SB bodies, fastly in the case of TL body (Fig. 3). The reason of changing behaviour of the perovskite pigment is related to the difference in the chemical and phase compositions of the porcelain stoneware bodies with a different amounts of liquid phase (Fig. 4).

The perovskite pigment is more stable in the conventional porcelain stoneware (BA) with liquid phase contents between 65% and 75% at different varying firing times. In contrast, the pigment dissolution in the SB and TL bodies was faster than in the BA body. The pigment dissolution in the SB body is not linearly correlated to the firing time, due to the rapid increase of the amount of liquid phase with increasing the soaking time (Fig. 4, and 5). Although the amount of undissolved pigment is high after 5 minutes, the colour efficiency needs more than 15 minutes soaking time due to the exponential increase of the vitreous phase with time (Fig. 4). The TL exhibits the fastest pigment dissolution due to the high content of CaO and ZnO in the liquid phase.^{18,27} The percentage of residual perovskite in the TL body is found very low after the short soaking time. Interesting enough, the red

colour is surprisingly intense despite the low pigment percentage, due to the optimal content (65%) of glassy phase (65%) (Fig. 5).

As shown in figure 6, the variation of the a^* parameter is linearly correlated with the amount of undissolved perovskite in the BA and TL bodies, while in the case of the SB body the correlation is not linear. This discrepancy is due to the fact that the pigment colouring efficiency is not only related to the amount of undissolved perovskite but also to the content of liquid phase formed.^{28,29}

As a matter of fact, the high values of the a^* -to-perovskite ratio correspond to higher contents of vitreous phases in the body (Fig. 7). Therefore, the higher the content of vitreous phases, the higher the pigment colouring efficiency and the faster the pigment dissolution rate. The high content of liquid phase enhances the chemical reactivity and ability for wetting the pigment particles.

So, the interactions among perovskite pigment and porcelain stoneware are mostly affected by the phase composition of the bodies. Also, the values of viscosity, surface tension and refractive index of the different liquid phases for the different bodies showed quite similar values (Table 1).

Technological behaviour in glazes and frits

Colour development in glazes and frits—In order to test the colour development of the perovskite pigment, the pigment was added to five ceramic coatings (two frits and three glazes) having different contents of reactive oxides (i.e. B_2O_3 , CaO, MgO, PbO, ZnO) (Table 2).

The pigment colouring efficiency varies with increasing firing temperature and soaking time (Figs. 8-9). Perovskite develops an excellent colour purity in both frits (F1 and F2) and porcelain stoneware glaze (S1) even after 45 minutes soaking. In particular, F1 shows the best result if compared to F2 and S1, despite its lower surface tension. The different behaviour of S1 and F2 can be explained by the fact that the former develops a relatively large amount of crystalline phases and the difference in the contents of oxides, such as PbO, ZnO and B_2O_3 (Table 2).

The pigment colouring efficiency in both frits decreased when samples were fired over 1100 °C, while in the S1 glaze the red colour remained stable up to 1200 °C and 45 minutes soaking (Fig. 9).

The pigment colouring efficiency is lower in the glazes S2 and S3, as confirmed by lower values of a^* compared with the two frits or the glaze S1. This fact is mostly due to the large amount of crystalline phases: ~20% wt. in the glaze S2 (anorthite → gehlenite → clinopyroxene → quartz) and ~40% wt. in these glaze S3s (zircon → anorthite → quartz Table 2). The red colour of these coatings remains stable with increasing both firing temperature and soaking time, showing an increase of pigment dissolution only after 45 minutes soaking (Fig. 8).

The linear correlation between the red colour of glazes and the perovskite content is clearly appreciable in figure 10, with the following exceptions:

- a) different values of a^* for the same amount of perovskite (i.e. 1.5-2%) implying that the pigment colouring efficiency is not only affected by the pigment amount, but also by the chemical and phase composition of coating;
- b) a non-linear increase of the a^* values for high amounts of pigment maybe related to colour saturation;
- c) a tendency to develop a greenish shade when the pigment is completely dissolved in the glaze is explained by the different coordination and ligand environment of chromium in perovskite and boro-silicate glass.^{30,31}

The pigment dissolution mechanism was performed through SEM observations and EDS microanalysis. Results showing that pigment particles decrease in size and have less clean-cut outlines with increasing firing temperature in both frits (F1 and F2 (Fig. 11)). In

particular, grain boundaries appear to be corroded after 45 minutes soaking, but this enhanced dissolution did not affect the colouring efficiency, because the mean particle size of pigment remained coarser than 5-7 μm , that is a sufficient value to bestow a red colour on the coating.

In the porcelain stoneware glaze (S1) the pigment particle size did not decrease with increasing soaking time at 1200 °C. The well defined grain boundaries observed after 5 minutes soaking (Fig. 11A12A) become gradually less sharp and particles appear less homogeneous after a soaking time of 15 minutes (Fig. 11B12B). Perovskite grains are almost completely corroded after 45 minutes soaking (Fig. 11C12C). The chemical dissolution did not apparently affect the pigment colour efficiency, that remained the same even after 45 minutes of soaking time (Fig. 8).

As regards the glaze for single-fired light-coloured stoneware (S2) for increasing soaking times (from 5 to 45 minutes at 1150°C) the particle size of perovskite decreased down to 5 μm and the grain boundaries appeared more or less extensively corroded. This observation confirmed the phase composition data and explained the significant decrease of colouring efficiency with increasing firing time.

In the case of the monoporosa glaze (S3) the particle size is below 5 μm already after 5 minutes soaking, while for longer times (15 and 45 minutes) the pigment particles were no longer detected at SEM, notwithstanding powder diffraction patterns revealed a tiny amount of residual perovskite.

4. Conclusions

The colour development of red perovskite $\{\text{Y}(\text{Al},\text{Cr})\text{O}_3$ perovskite} pigment in different ceramic bodies and glazes was evaluated by colourimetric and powder diffraction analyses after firing at different temperatures and soaking time.

The pigment is fully stable at the appropriate firing temperature in double-fired wall tiles at 1150 °C.

In glazes for light-coloured stoneware floor tiles and *monoporosa* wall tiles, the pigment is chemically attacked and partially dissolved, due to the higher content of zinc and calcium in the liquid phase at temperatures over 1100 °C. Moreover, the pigment shows a low colouring efficiency that is justified by the particularly high amount of crystalline phases formed in the glaze during firing.

The perovskite stability is satisfactory up to 1200 °C even for long soaking times (e.g. 45 minutes) in glazes for porcelain stoneware tiles free of zinc and lead.

The perovskite pigment is stable in both the conventional and ultrawhite porcelain stoneware bodies up to 1200°C even for long soaking times. In contrast, it is rapidly dissolved in translucent bodies, due to large contents of calcium, zinc and magnesium oxides in their liquid phase.

The pigment dissolution is affected not only by firing temperature and soaking time, but mostly by the chemical composition of the liquid phase formed in both bodies and glazes. In particular, the pigment dissolution rate is directly correlated to the content of chemically reactive components, such as calcium, magnesium, zinc and lead oxides.

On the other hand, the colouring efficiency is related to the amount and particle size of undissolved perovskite as well as to the phase composition of the ceramic matrices.

The red perovskite pigment $\text{YAl}_{1-x}\text{Cr}_x\text{O}_3$ is stable in most ceramic applications and ensures an excellent colour efficiency, in particular in porcelain stoneware glazes and bodies up to 1250 °C of firing temperature. In strongly aggressive glazes (i.e. those rich in calcium, magnesium, zinc and lead oxides). The perovskite dissolution is relatively fast, so that the pigment colouring efficiency is compromised for long firing times, though it appears to be

~~in any case satisfactory for the very short soaking (<5 minutes) currently applied in the tilemaking industry.~~

~~Acknowledgements~~

~~We Authors wish to~~ thank the European Synchrotron Radiation Facility (ESRF) for providing access to synchrotron radiation under the public beamtime programme (exp. No. CH1321). ~~S;~~ special thanks to BM1 (the Swiss-Norwegian Beam Lines) staff for the kind assistance during data collections.

References

- 1] F. Bondioli, T. Manfredini and G.C. Pellacani, *Interceram* **48** (1999) 414-22.
- 2] A.L. Costa, G. Cruciani, M. Dondi and F. Matteucci, *Industrial Ceramics* **23** (2003) 1-11.
- 3] A. Garcia, M. Llusar, J. Calbo, M.A. Tena and G. Monros, *Green Chemistry* **3** (2001) 238-42.
- 4] V.L. Lavilla and J.M. Lopez Rincon, *Br. Ceram. Trans.* **80** (1981) 105-08.
- 5] H.D. De Ahna, *Ceram. Eng. Sci. Proc.* **1** (1980) 860-62.
- 6] A. Escardino, S. Mestre, A. Barba, M. Monzon, P. Jodar and L. Diaz, *Qualicer 2002 P.GI* (2002) 271-82.
- 7] F. Lamilla, *Ceram. Eng. Sci. Proc.* **10-1/2** (1989) 49-51.
- 8] F. Bondioli, A.B. Corradi, A.M. Ferrari, C. Leonelli, C. Siligardi, T. Manfredini, N.G. Evans, J. *Microwave Power and Electromagnetic Energy* **33** (1998) 18-23.
- 9] G. Baldi, M. Bitossi and V. Del Conte, *International Patent PCT/EP96/01028, WO 96/28384G.*
- 10] G. Baldi and N. Dolen, *Mat. Eng.* **10** (1999) 151-64.
- 11] G. Baldi, N. Dolen, A. Barzanti and V. Faso, *Key Eng. Mat.* **264-268** (2004) 1545-48.
- 12] F. Matteucci, G. Cruciani, M. Dondi, G. Baldi and A. Barzanti, *Key Eng. Mat.* **264-268** (2004) 1549-52.
- 13] R.A. Eppler, *Am. Ceram. Soc. Bull.* **66** (1987) 1600-04.
- 14] F. Matteucci G. Cruciani, M. Dondi, G. Guarini and M. Raimondo, *Qualicer 2004 P.GI.* (2004) 261-72.
- 15] R.H. Mitchell, *Perovskites – Modern and ancient*, (Almaz Press – Thunder Bay, Appen, 2002) p. 318.
- 16] G. Cruciani, F. Matteucci, M. Dondi, G. Baldi, A. Barzanti, in preparation.
- 17] Y. Marinova, J.M. Hohemberger, E. Cordoncillo, P. Escribano and J.B. Carda, *J. Eur. Ceram. Soc.* **23** (2003) 213-20.
- 18] Italian Ceramic Society, in “Colour, pigments and colouring in ceramics” (SALA, Modena, 2003) p. 295.
- 19] A.C. Larson, R.B. Von Dreele, *Los Alamos National Laboratory Report LAUR.* (2000) 86-748.
- 20] B.H. Toby, *J. Appl. Cryst.* **34** (2001) 210-13.
- 21] R. Diehl, G. Brandt, *Mat. Res. Bull.* **10** (1975) 85-90.
- 22] T. Lakatos, L.G. Johansson and B. Skimmingskold, *Glass Technol.* **6** (1972) 88-95.
- 23] F. Cambier, A. Lérique, in *Vitrification, Processing of Ceramics*, Vol.17B, Part II, Weinheim, 1996, edited by R.W. Cahn, P. Haasen, E.J. Kramer, (VCH), p.123.
- 24] M. Ahmed and D.A. Earl, *Am. Ceram. Soc. Bull.* **81** (2002) 47-51.
- 25] M. Dondi, F. Matteucci, G. Cruciani, G. Baldi, A. Barzanti, in preparation.
- 26] S.H. Murdock, T.D. Wise and R.A. Eppler, *Ceram. Eng. Sci. Proc.* **10** (1989) 55-64.
- 27] D.R. Eppler and R.A. Eppler, *Ceram. Eng. Sci. Proc.* **18** (1997) 139-49.
- 28] D.R. Eppler and R.A. Eppler, *Ceram. Eng. Sci. Proc.* **19** (1998) 17-37.
- 29] F. Buchanan, R.J. Taylor and J.G. Helliwell, *Brit. Ceram. Trans.* **97** (1998) 83-86.
- 30] C.P. Poole Jr., *J. Phys. Chem. Solids* **25** (1964) 1169-82.
- 31] F. Rasheed, K.P. O'Donnell, B. Henderson and D.B. Hollis, *J. Phys. Condens. Matter* **3** (1991) 1915-30.

Table 1 Chemical composition of porcelain stoneware bodies and chemico-physical properties of the liquid phase formed at high temperature²²⁻²³

<u>% weight</u>	<u>Conventional (BA)</u>		<u>Ultrawhite (SB)</u>		<u>Translucid (TL)</u>	
	<u>Body</u>	<u>Liquid phase</u>	<u>Body</u>	<u>Liquid phase</u>	<u>Body</u>	<u>Liquid phase</u>
<u>SiO₂</u>	<u>71.2</u>	<u>67.8</u>	<u>65.7</u>	<u>76.1</u>	<u>71.3</u>	<u>74.4</u>
<u>TiO₂</u>	<u>0.5</u>	<u>1.0</u>	<u>0.1</u>	<u>0.2</u>	<u>0.1</u>	<u>0.1</u>
<u>ZrO₂</u>	<u><0.1</u>	<u><0.1</u>	<u>7.2</u>	<u>0.1</u>	<u><0.1</u>	<u><0.1</u>
<u>Al₂O₃</u>	<u>15.8</u>	<u>17.3</u>	<u>16.5</u>	<u>10.7</u>	<u>14.9</u>	<u>12.9</u>
<u>Fe₂O₃</u>	<u>0.5</u>	<u>1.1</u>	<u>0.1</u>	<u>0.2</u>	<u>0.1</u>	<u>0.2</u>
<u>MgO</u>	<u>0.5</u>	<u>1.0</u>	<u>0.2</u>	<u>0.5</u>	<u>1.7</u>	<u>2.4</u>
<u>CaO</u>	<u>0.7</u>	<u>1.1</u>	<u>1.7</u>	<u>2.5</u>	<u>4.9</u>	<u>5.0</u>
<u>ZnO</u>	<u><0.1</u>	<u><0.1</u>	<u><0.1</u>	<u><0.1</u>	<u>0.5</u>	<u>0.7</u>
<u>Na₂O</u>	<u>3.2</u>	<u>5.6</u>	<u>3.3</u>	<u>5.6</u>	<u>1.4</u>	<u>1.7</u>
<u>K₂O</u>	<u>2.4</u>	<u>5.0</u>	<u>1.9</u>	<u>4.1</u>	<u>1.8</u>	<u>2.6</u>
<u>L.o.I.</u>	<u>3.4</u>	<u>=</u>	<u>3.2</u>	<u>=</u>	<u>3.7</u>	<u>=</u>
<u>Temperature of max densification (°C)</u>	<u>1210</u>		<u>1210</u>		<u>1200</u>	
<u>Refractive index (1)</u>		<u>1.49</u>		<u>1.49</u>		<u>1.50</u>
<u>Viscosity at 1200 °C (kPa s)</u>		<u>4.4</u>		<u>4.1</u>		<u>4.4</u>
<u>Surface tension at 1200 °C (mN m⁻¹)</u>		<u>330</u>		<u>320</u>		<u>340</u>

Table 2 Chemical and phase composition and main physical properties of frits (F1 and F2) and glazes (S1, S2 and S3)

<u>Component / Property</u>	<u>Unit</u>	<u>F1</u>	<u>F2</u>	<u>S1</u>	<u>S2</u>	<u>S3</u>
<u>SiO₂</u>	<u>% wt.</u>	<u>63.9</u>	<u>57.1</u>	<u>53.5</u>	<u>51.1</u>	<u>49.7</u>
<u>ZrO₂</u>		<u><0.1</u>	<u><0.1</u>	<u><0.1</u>	<u><0.1</u>	<u>8.1</u>
<u>B₂O₃</u>		<u>11.7</u>	<u>8.9</u>	<u><0.1</u>	<u>1.2</u>	<u>2.4</u>
<u>Al₂O₃</u>		<u>9.5</u>	<u>9.0</u>	<u>25.2</u>	<u>22.6</u>	<u>19.7</u>
<u>MgO</u>		<u><0.1</u>	<u>1.1</u>	<u>3.4</u>	<u>1.4</u>	<u>0.2</u>
<u>CaO</u>		<u>0.5</u>	<u>7.9</u>	<u>8.9</u>	<u>13.5</u>	<u>12.6</u>
<u>ZnO</u>		<u>1.0</u>	<u>5.0</u>	<u><0.1</u>	<u>5.1</u>	<u><0.1</u>
<u>BaO</u>		<u><0.1</u>	<u>1.4</u>	<u><0.1</u>	<u>1.4</u>	<u>3.2</u>
<u>PbO</u>		<u>5.5</u>	<u>2.7</u>	<u><0.1</u>	<u>0.9</u>	<u><0.1</u>
<u>Na₂O</u>		<u>6.1</u>	<u>2.0</u>	<u>5.6</u>	<u>2.6</u>	<u>2.2</u>
<u>K₂O</u>		<u>1.1</u>	<u>4.1</u>	<u>3.0</u>	<u>0.6</u>	<u>1.3</u>
<u>Zircon ZrSiO₄</u>	<u>% wt.</u>	<u>=</u>	<u>=</u>	<u>=</u>	<u>=</u>	<u>~5</u>
<u>Quartz α -SiO₂</u>		<u>=</u>	<u>=</u>	<u><1</u>	<u>~10</u>	<u>~5</u>
<u>Anorthite CaAl₂Si₂O₈</u>		<u>=</u>	<u>=</u>	<u>~5</u>	<u>~15</u>	<u>~5</u>
<u>Wollastonite CaSiO₃</u>		<u>=</u>	<u>=</u>	<u>~5</u>	<u>~10</u>	<u>=</u>
<u>Gehlenite Ca₂Al₂SiO₇</u>		<u>=</u>	<u>=</u>	<u><1</u>	<u>~10</u>	<u>=</u>
<u>Temperature of softening T₁</u>	<u>°C</u>	<u>930</u>	<u>940</u>	<u>1210</u>	<u>1150</u>	<u>1100</u>
<u>Temperature of half sphere T₂</u>		<u>1265</u>	<u>1180</u>	<u>1275</u>	<u>1200</u>	<u>1195</u>
<u>Temperature of melting T₃</u>		<u>1290</u>	<u>1230</u>	<u>1305</u>	<u>1235</u>	<u>1230</u>
<u>Refractive index</u>	<u>1</u>	<u>1.505</u>	<u>1.540</u>	<u>1.525</u>	<u>1.545</u>	<u>1.560</u>
<u>Viscosity at T₁</u>	<u>MPa s</u>	<u>4.90</u>	<u>4.95</u>	<u>4.65</u>	<u>4.95</u>	<u>5.25</u>
<u>Surface tension at T₁</u>	<u>mN m⁻¹</u>	<u>295</u>	<u>325</u>	<u>380</u>	<u>395</u>	<u>385</u>

Table 3 Firing temperatures of the different ceramic substrates

<u>°C</u>	<u>Frits</u>		<u>Glazes</u>			<u>Porcelain stonewares</u>		
	<u>F1</u>	<u>F2</u>	<u>S1</u>	<u>S2</u>	<u>S3</u>	<u>BA</u>	<u>SB</u>	<u>TL</u>
<u>950</u>	X	X						
<u>1000</u>					X			
<u>1050</u>	X	X		X	X			
<u>1100</u>				X	X			
<u>1150</u>	X	X	X	X				
<u>1200</u>			X			X	X	X
<u>1250</u>			X					

Table 4 Refinement and unit cell parameters of the pigment $\text{YAl}_{0.965}\text{Cr}_{0.035}\text{O}_3$. Figures in parentheses are standard deviations in the last decimal figure.

<u>Unit-cell dimensions</u>	<u>Unit</u>	<u>Mean value</u>
<u>Parameter <i>a</i></u>	<u>Å</u>	<u>5.33160(3)</u>
<u>Parameter <i>b</i></u>	<u>Å</u>	<u>7.37725(4)</u>
<u>Parameter <i>c</i></u>	<u>Å</u>	<u>5.18411(2)</u>
<u>Metal-ligand distance in the B site</u>		
<u>Al-O₁</u>	<u>Å</u>	<u>1.899(1)</u>
<u>Al-O₂</u>	<u>Å</u>	<u>1.922(1)</u>
<u>Al-O₃</u>	<u>Å</u>	<u>1.907(1)</u>
<u>Rietveld refinements</u>		
<u>Number of data</u>	<u>1</u>	<u>10794</u>
<u>R_{Bragg} (perovskite)</u>	<u>1</u>	<u>0.039</u>
<u>R_{wp}</u>	<u>1</u>	<u>0.154</u>

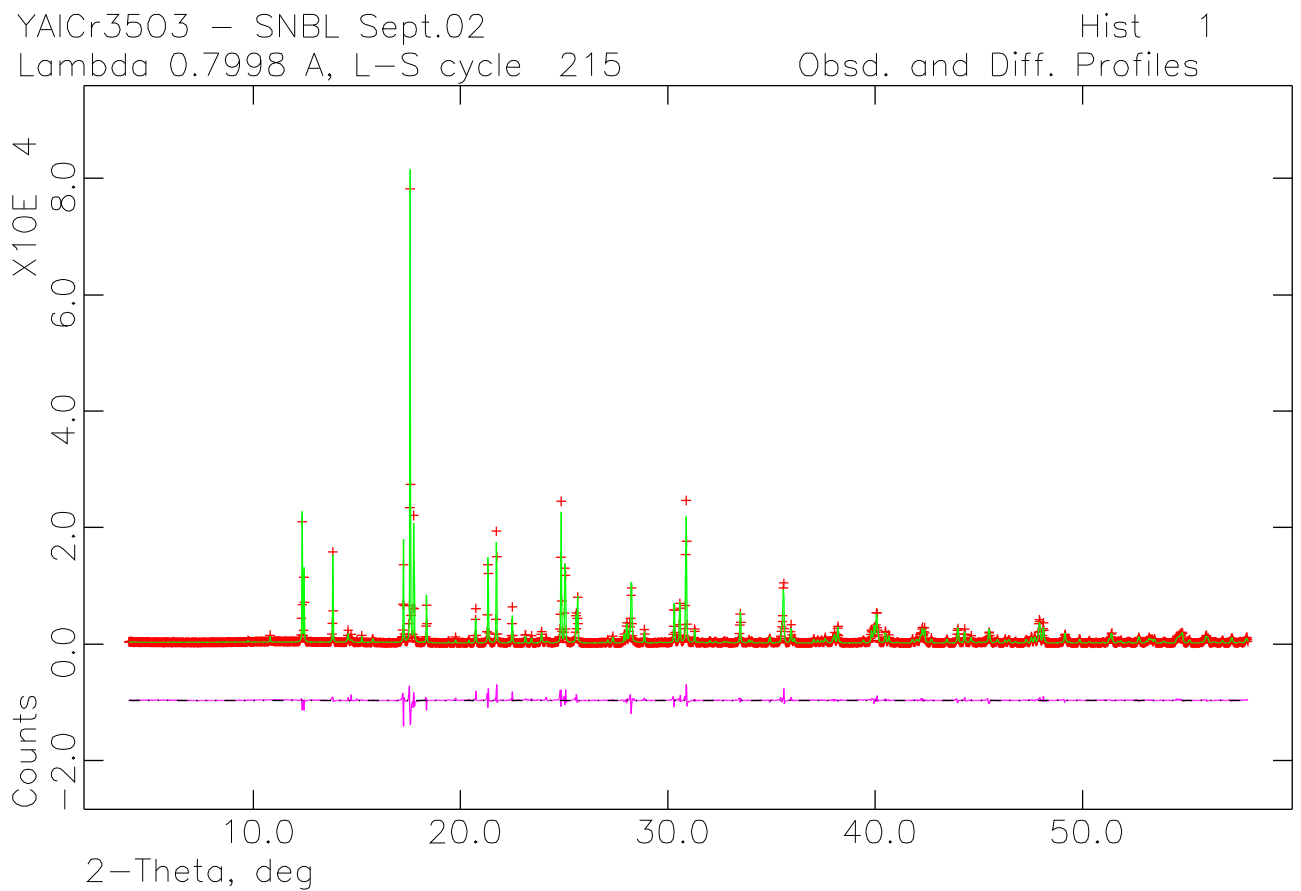
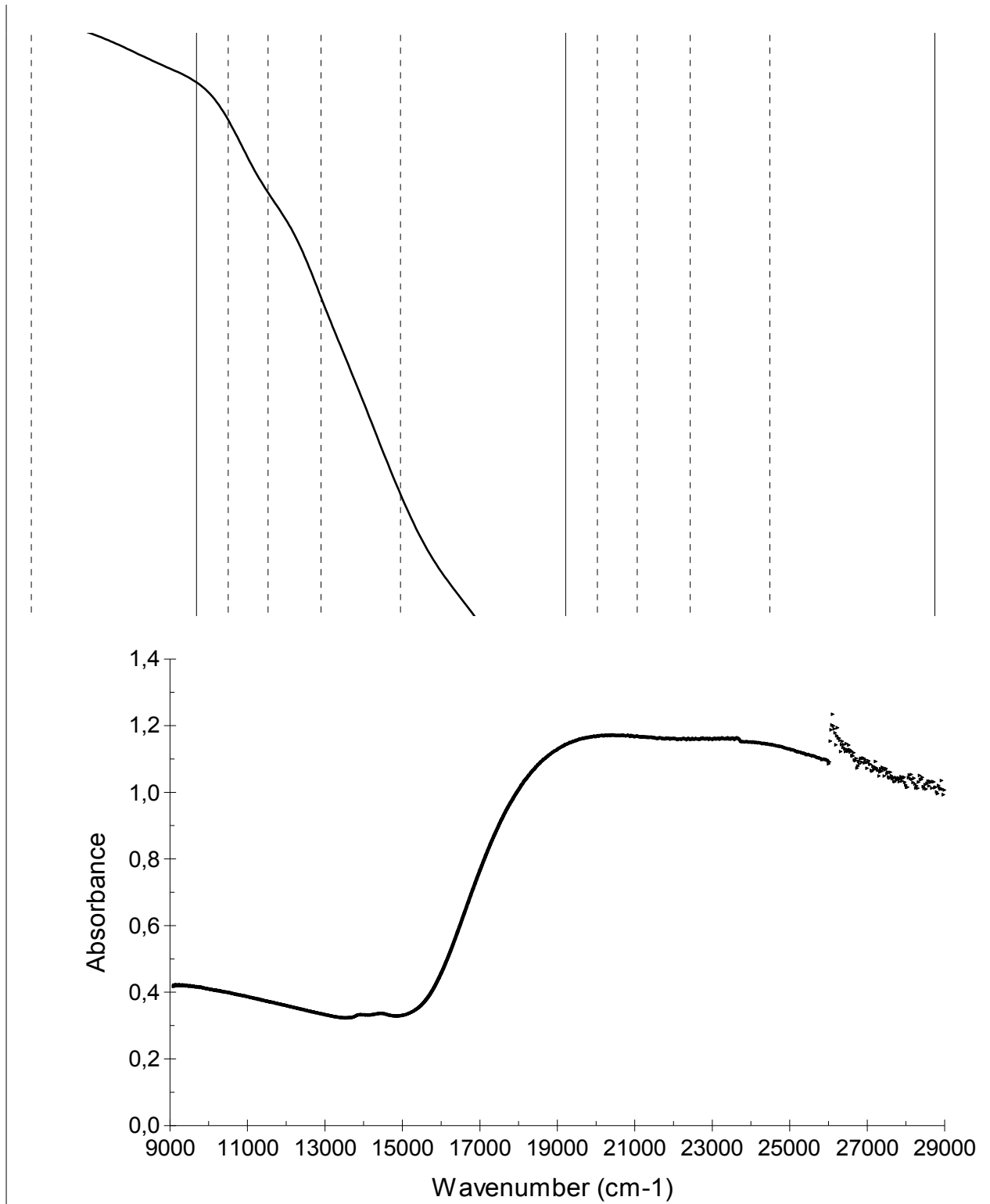
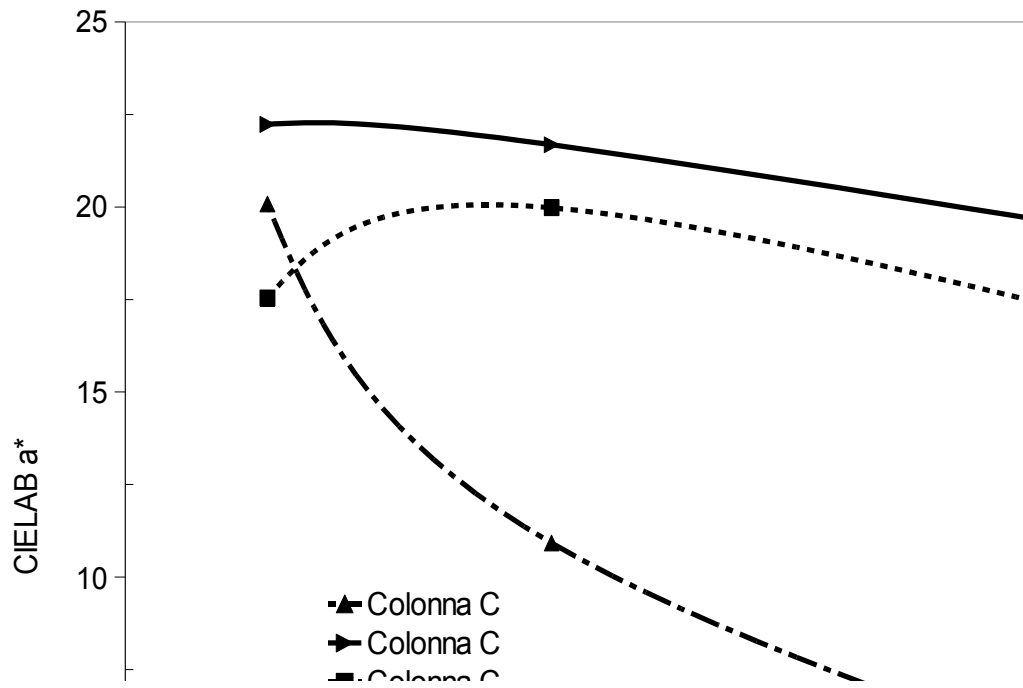


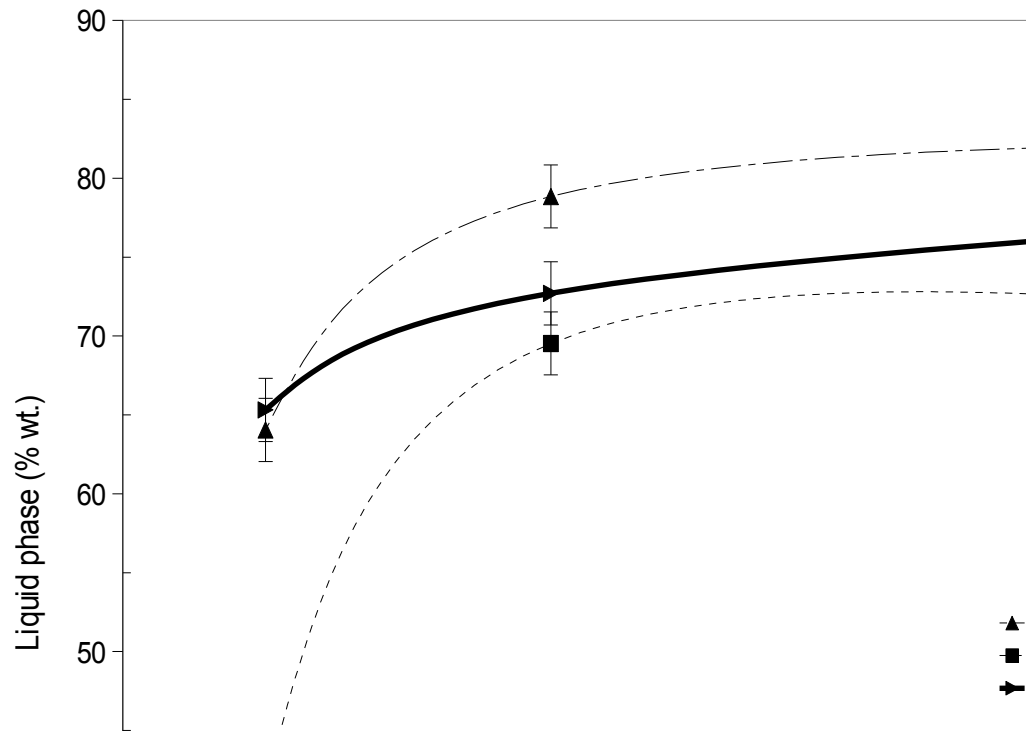
Fig. 1. Rietveld refinement plot of the X-ray powder diffraction data of $\text{YAl}_{0.965}\text{Cr}_{0.035}\text{O}_3$. In the figure the continuous line represent the calculated pattern, while cross points show the observed pattern. The difference curve between observed and fitted profiles is plotted below.



[2](#)—[Fig. 2.](#) Particle size distribution (A) and diffuse reflectance spectrum (B) of the perovskite pigment.



[Fig. 3. Red hue variation \(a*\) vs. soaking time \(minutes\) in the different porcelain stoneware bodies fired at 1200°C](#)



[4](#)—[Fig. 4.](#) Liquid phase amount (% wt.) vs. soaking time at 1200°C in minutes (min) in the different porcelain stoneware bodies.

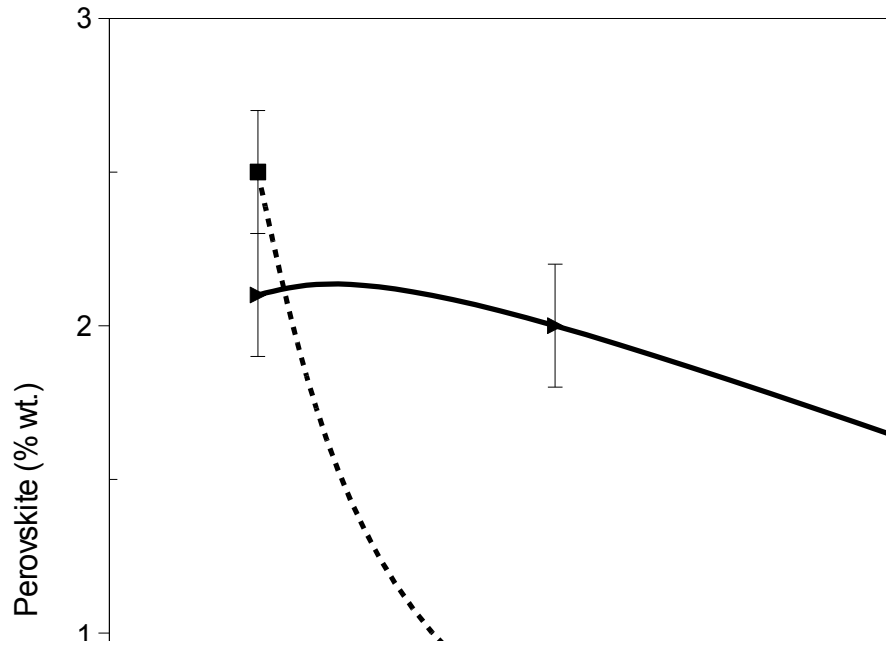


[Fig. 5.](#) — Amount of perovskite undissolved (% wt.) vs. soaking time at 1200°C in minutes (min) in the different porcelain stoneware bodies.



[6](#) — [Fig. 6.](#) Red hue variations (a^*) vs amount of perovksite undissolved (% wt.) in the different porcelain stoneware bodies.

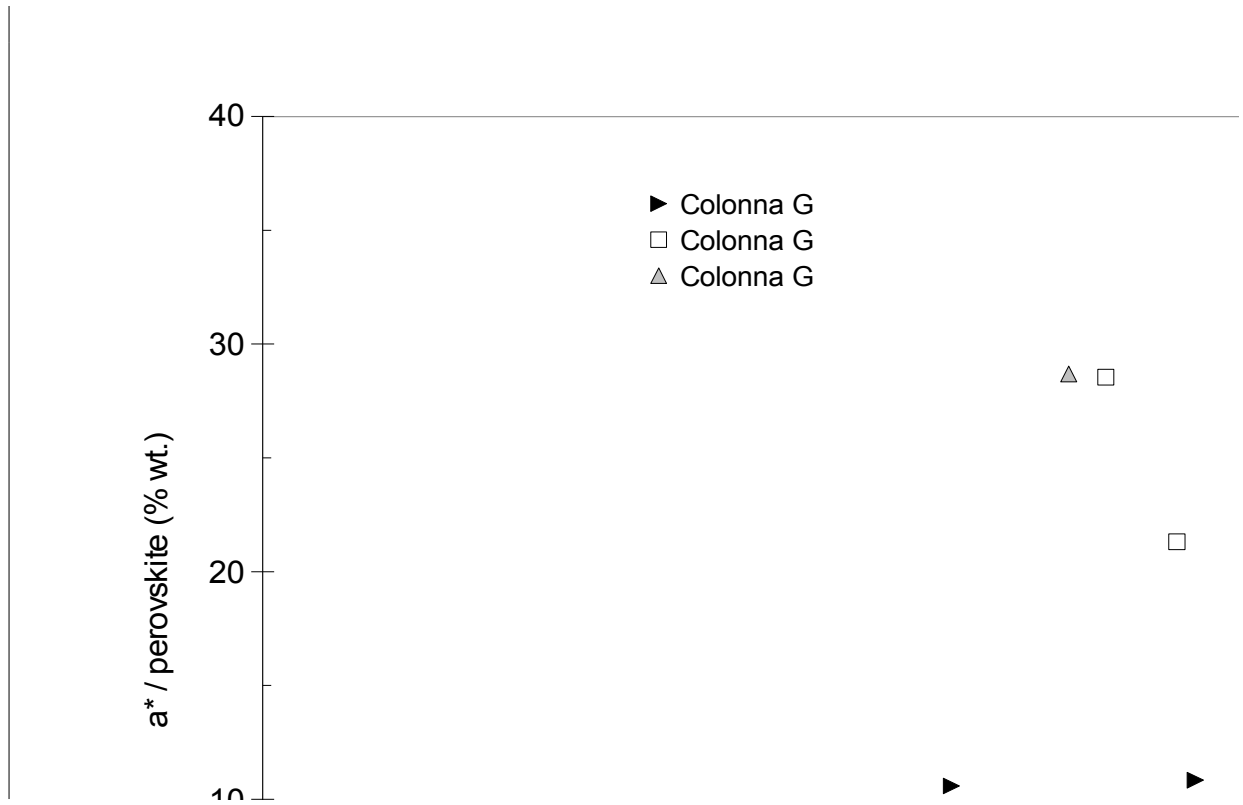


[Fig. 7. 7](#) — Pigment colouring efficiency (i.e. $a^*/\text{perovskite \% wt.}$) vs. liquid phase amount (% wt.) in the different porcelain stoneware bodies.

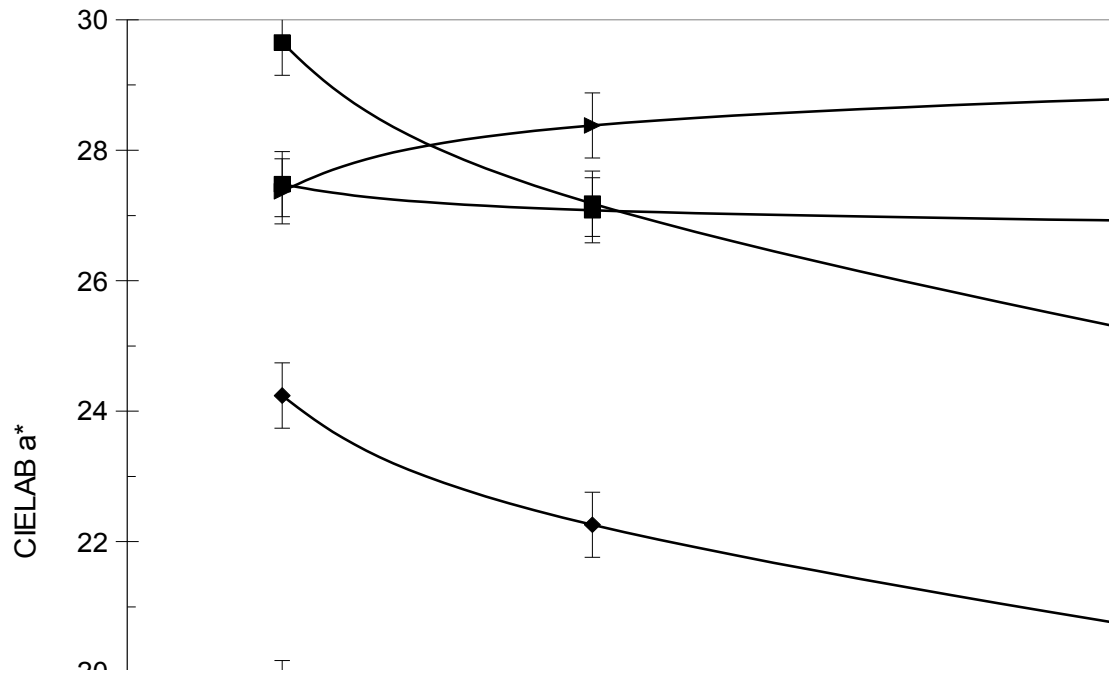
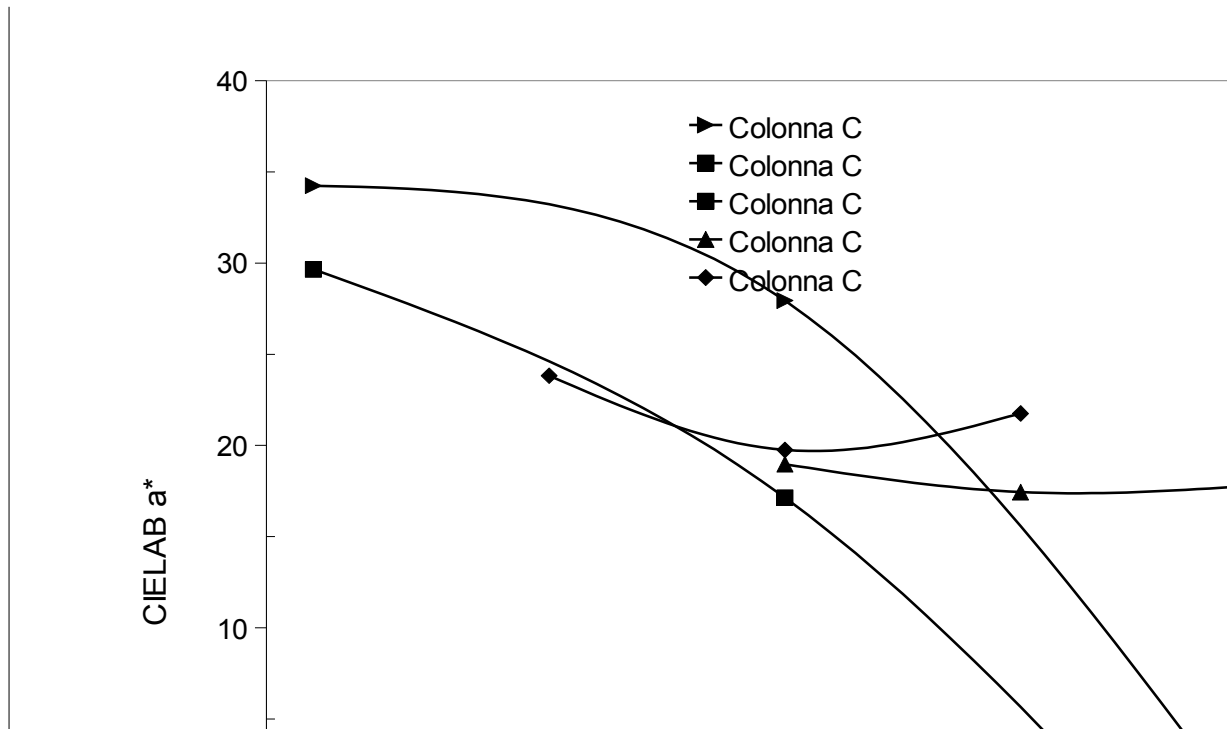


[Fig. 8-](#) Red hue variations (a^*) vs. soaking time in the different frits (F1 and F2) and glazes (S1, S2 and S3).



9—Fig. 9. Red hue variations (a^*) vs. maximum firing temperature in the different frits (F1 and F2) and glazes (S1, S2 and S3) after 5 minutes of soaking time.

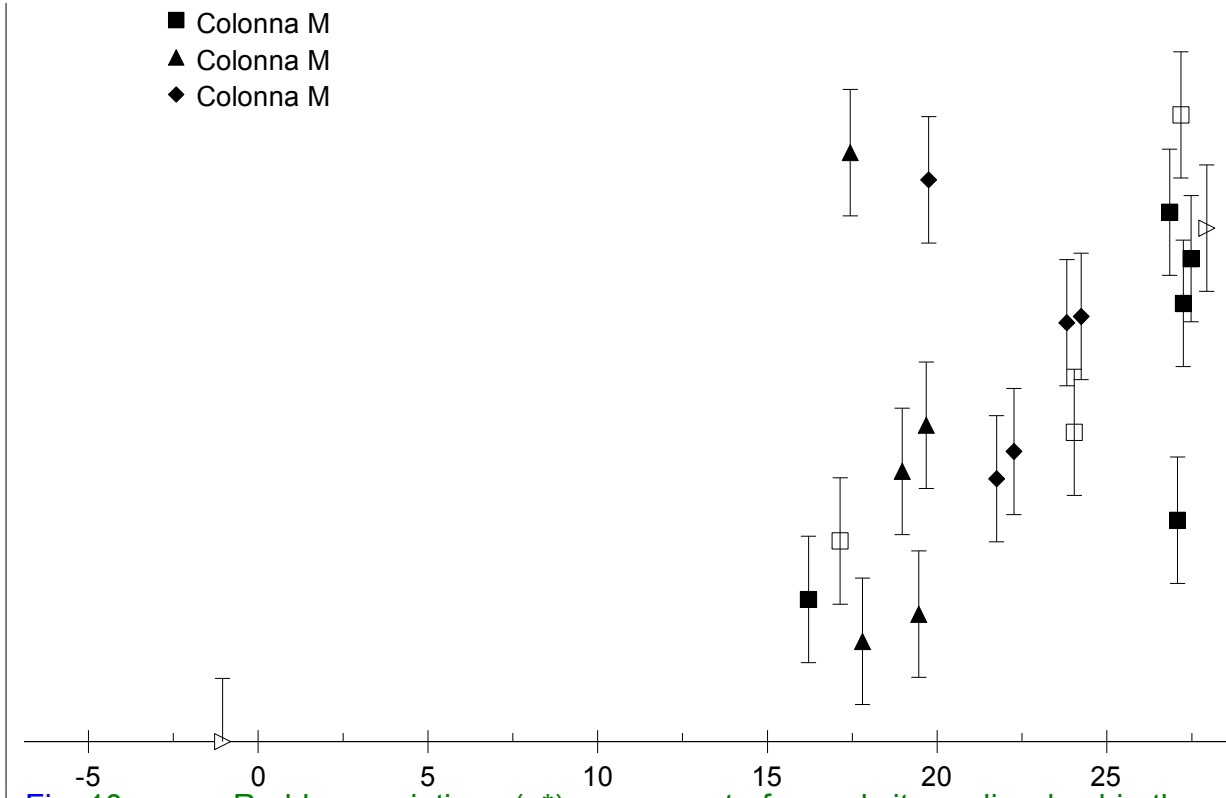
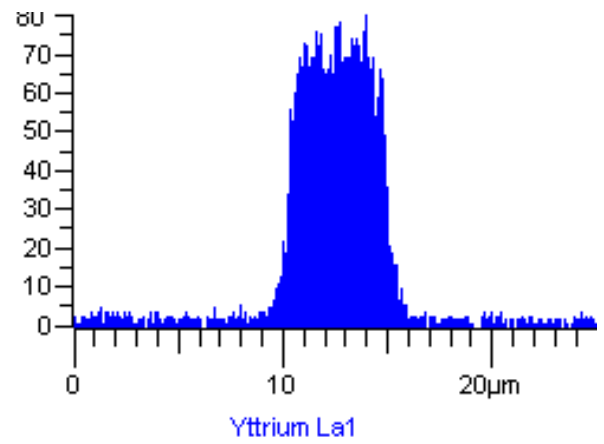
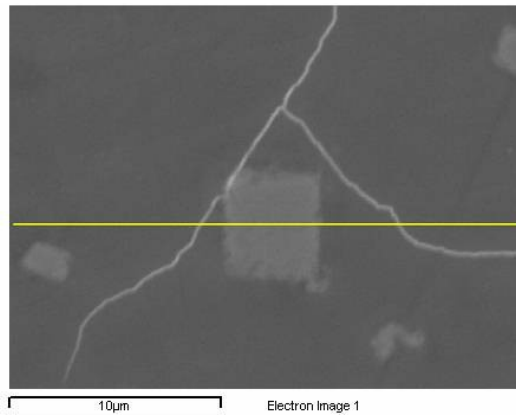


[Fig. 10](#) ——. Red hue variations (a^*) vs. amount of perovskite undissolved in the different frits (F1 and F2) and glazes (S1, S2 and S3).

A



B

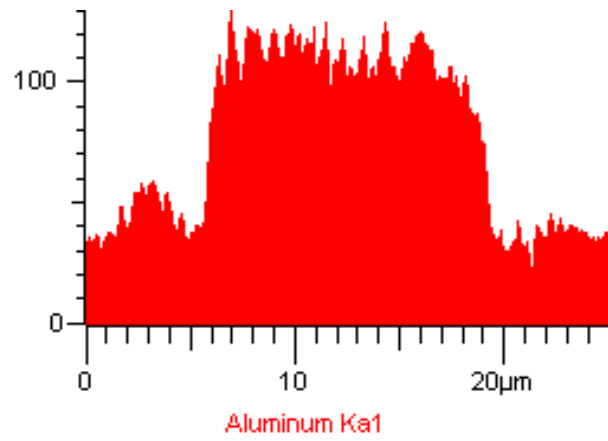
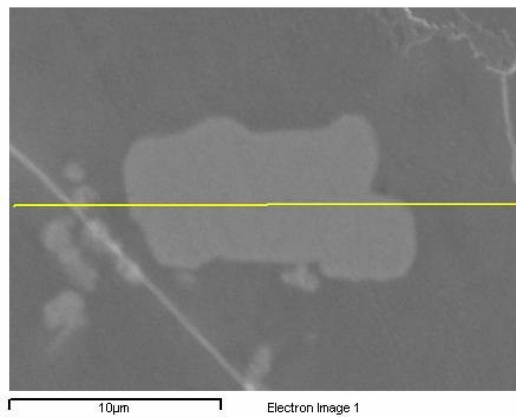


Fig. 11. SEM observations and EDS line scans of the perovskite pigment into the F2 frit fired at 950°C for 5 minutes (A) and 45 minutes of soaking time (B).

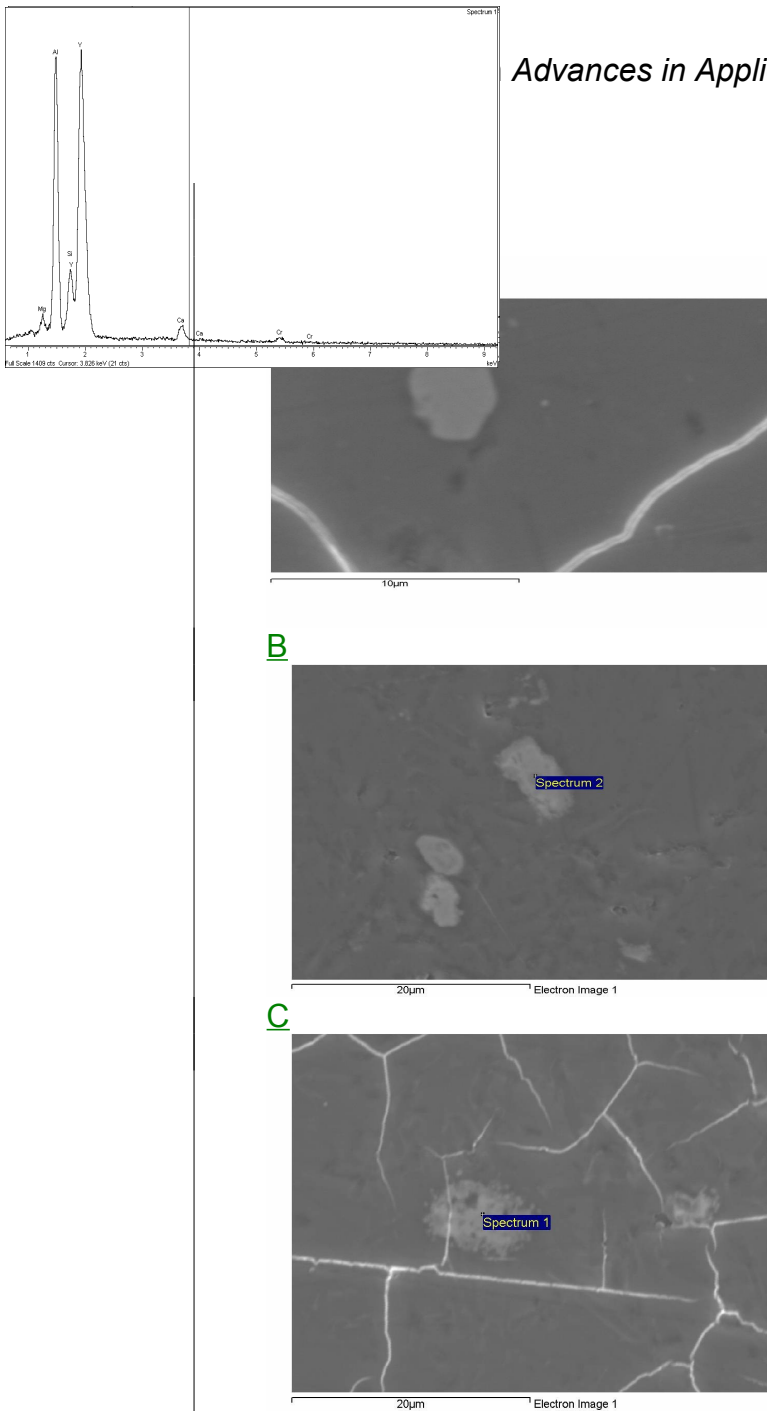


Fig. 12. SEM observations and EDS spectra of the perovskite pigment into the glaze S1 fired at 1200°C for varying soaking time: 5 (A), 15 (B) or 45 minutes (C).